



Development of an automated system for electrochemical production of coagulant based on photocolorimetric analysis

Andrii Safonyk , Ivanna Hrytsiuk , Marko Klepach ,
Maksym Mishchanchuk , Andriy Khrystyuk 

National University of Water and Environmental Engineering, Institute of Automatics, Cybernetics and Computer Engineering, Soborna St, 11, Rivne, Rivnens'ka oblast, 33028, Ukraine

RECEIVED 16.02.2021

REVIEWED 05.04.2021

ACCEPTED 24.05.2021

Abstract: The article describes the development of a model problem for electrocoagulation treatment of industrial wastewater taking into account changes in voltage and current. The study included computer simulation of the change in the concentration of iron at the output of the electrocoagulator at variable current levels. The laboratory-scale plant was developed for the photocolorimetric analysis of the iron-containing coagulant. It consisted of a flowing opaque cell through which water is pumped with a constant flow and also the block for processing and storage of information. Such structure allows to reduce human participation in the measurement process and to ensure the continuity of measurement without any need for sampling of the tested material, as well as to reduce the measurement cost. During the processing of results, graphical dependences were determined between RGB-components of water colour and the corresponding concentration of total iron and Fe^{3+} in water.

Keywords: coagulant, colour of water, electrocoagulation process, photocolorimetric method, RGB, total iron, wastewater treatment

INTRODUCTION

The development of technology and demand for goods and natural resources have led to increased pollution of the aquatic environment and the environment in general. Therefore, many scientists and environmentalists promote programmes designed to improve the aquatic environment and the state of the ecosystem. Currently, water quality has declined dramatically, which has a detrimental effect on aquatic ecosystems, nature, and people. All this leads calls for the implementation of wastewater treatment and control techniques and methods. The effectiveness of any treatment method is characterised by the quality, time required to perform the process, and the use of resources and certain other parameters.

In practice, small treatment plants that use reagents are increasingly often applied for water purification. Wastewater treatment plants fitted with such solutions are especially relevant for agriculture, light industry, etc. However, the use of reagents

requires their supply and storage. Electrochemical methods allow to obtain reagents on-site from raw materials available. One such method is electrocoagulation. The application of electrocoagulation in wastewater treatment is advanced. It has been used for many years and continues to be developed. Recently, a growing attention is paid to the study of the process using mathematical modelling, as it helps to improve equipment design, reduce operating costs, and predict the efficiency of the process in a wide range of operation conditions with minimal production costs. Besides, relevant research provides a basis for the development of automated systems that control electrocoagulation processes. As in other similar cases, the process of obtaining coagulant by electrocoagulation involves complex and expensive field experiments to determine the content of the useful element (i.e. iron) in the coagulant. One of laboratory methods to determine iron content in coagulant is the photocolorimetry. The development of technologies for the absorption of light by a conditioned substance in the visible spectrum, converting light energy into

electrical energy, the so-called photocolorimetry technology, allows us to assess the quality of multicomponent compounds with greater accuracy and speed. Moreover, standardised methods for the determination of the iron content in water include photocolorimetric analysis. With the increase in the iron concentration, we observe a change in the colour intensity of water samples examined and the optical density of the medium.

Most aspects of electrocoagulation wastewater treatment have not been sufficiently studied and are subject to ongoing improvements. Many authors (ASSEMIAN, KOUASSI [2018]; POSAVČIĆ *et al.* [2019], FORERO *et al.* [2020]) focus on such parameters as pH, temperature, concentration of pollutants, whereas as pay little attention to the colour of the substance. Research by YASRI *et al.* [2020], KHANDEGAR *et al.* [2018] and PERREN *et al.* [2018] considers the basic principles of continuous wastewater treatment and the development of appropriate models that focus on different types of pollutants under various operating conditions. The study describes experiments carried to evaluate the efficiency of wastewater treatment, which includes measurements of turbidity, pH, conductivity, temperature, and oxygen saturation [FORERO *et al.* 2020].

Research by RAHMAN *et al.* [2020] shows the development of a wastewater treatment model with electrocoagulation that takes into account optimal conditions for the continuous operation of the system at a variable current density. AL-BARAKAT *et al.* [2020] describe the current distribution and fluid flow by modelling them as a diffusion process and conduct field and computer experiments to verify the adequacy of the model. Research by KOYUNCU, ARIMAN [2020] demonstrates the process of electrocoagulation and experiments on equipment operated in treatment plants, whereas YASRI *et al.* [2017] explores the degree and dispersion of contaminants formed on the plates at different times of electrocoagulation and polarity changes. GOVINDAN *et al.* [2019] continues the previous study and in his article describes visual experiments that demonstrate the change in sediments obtained by electrocoagulation on plates at alternating current and examines the sediment obtained at different states of the electrolyte.

In their studies, MASAWAT *et al.* [2016] developed a digital colorimeter to determine the iron content with a software application that registers colour components that preserve certain values of red, green and blue, as well as calculate the values of hue, saturation, brightness, and grey based on the standard colour theory. In their study, LUKA *et al.* [2017] developed an inexpensive portable device for colorimetric analysis in the field. SREENIVASAREDDY [2017] determines the concentration of iron in drinking water according to the regulations of the United States Environmental Protection Agency. The study by BARROS *et al.* [2016] used a webcam to determine the iron content in water based on digital image colourimetry. The main method of this study uses the regression of least squares to obtain a quadratic equation based on red, green, and blue hues, and colour saturation and brightness, which allows to provide the most accurate analysis. The research of FIRDAUSA *et al.* [2014] focuses on comparing two methods to determine the concentration of chromium (Cr) and iron (Fe), and while the first method is based on a simple linear regression of a single colour R (red), G (green) or B (blue), the second method is based on the theory of least squares of all three colours R, G and B. However, all these works are based on field experiments, whereas concentrations of the

useful elements are determined in the laboratory. This is time consuming and costly in terms of materials used.

In accordance with the above, the development of an automated system is urgently needed to support electrochemical production of coagulant based on photocolorimetric analysis.

MATERIALS AND METHODS

To design an experimental device, it is necessary to synthesise a mathematical model that describes the process of industrial wastewater electrocoagulation while taking into account changes in voltage and current. This, in turn, makes it possible to compare the results of theoretical research with experimental data, as well as to assess the compliance of the electrocoagulation model with real data. Given that the concentration of iron in water changes the solution colour and its intensity, the experimental device for laboratory studies was used to supplement the digital subsystem for colour and light intensity analysis. To explore the process of electrocoagulation liquid treatment, we generalise the mathematical model developed by BOMBA and SAFONYK [2013] taking into account considerations described by BOMBA *et al.* [2016], SAMIR *et al.* [2016], KAUR and AMIT [2018] and YAVUZ, ÖGÜTVEREN [2018]. This formulation takes into account processes that take place in the reactor and affect the process, as well as the interaction of various factors: the concentration of suspended solids in water, applied current, flow speed and temperature of liquid, the external environment influence parameters, water in the reactor, and design parameters of the coagulator. Thus, to find the distributions of coagulant concentration C and temperature T in the electrocoagulator, we come to the following model problem:

$$\begin{cases} \frac{\partial C}{\partial t} = -v_C \nabla C + \nabla(D_C(T) \nabla C) + f_C(T)C + \Phi \\ \frac{\partial T}{\partial t} = -v_T \nabla T + D_T \Delta T + \Psi \end{cases}$$

$$\begin{aligned} C(x, 0) &= C_0(x), \quad T(x, 0) = T_0(x), \\ C(0, t) &= C^0(t), \quad T(0, t) = T^0(t), \end{aligned}$$

$$\left. \frac{\partial C}{\partial x} \right|_{x=l} = 0, \quad \left. \frac{\partial T}{\partial x} \right|_{x=l} = 0, \quad (2)$$

where: D_T = diffusion coefficients ($\text{m}^2 \cdot \text{s}^{-1}$), q_T = the intensity of internal heat sources, v_C = the speed of the coagulant propagation ($\text{m} \cdot \text{s}^{-1}$), v_T = temperature propagation speed ($\text{m} \cdot \text{s}^{-1}$), c_T = heat capacity ($\text{J} \cdot \text{kg}^{-1}$), ρ = density ($\text{kg} \cdot \text{m}^{-3}$), l = the length of the coagulator (m) ($0 < x < l$), H = the height of the coagulator (m), B = coagulator width (m).

During electrocoagulation, the electrolyte solution is heated. The amount of heat $\Psi = \frac{q_T}{c_T \rho}$, which is released, is proportional to the magnitude of the current, the time of its passage and the voltage drop $q_T = I \cdot U \cdot t$, U = applied voltage (V), I = current value (A), $f(T) = \eta \frac{3R_g T l}{8F d_b A_s P}$ = a function that takes into account the flotation component of the process [BOMBA, SAFONYK 2013], R_g = gas constant ($\text{J} \cdot (\text{mol} \cdot \text{K})^{-1}$), d_b = diameter of bubbles (m), P = atmospheric pressure (Pa), A_s = the cross-sectional area of the camera (m^2) and η = single bubble accumulation efficiency – is defined as the proportion of contaminant in the path of the bubble that actually sticks to the bubble.

Diffusion of particles in a liquid can be considered as a motion with friction, and the second Einstein relation can be applied to it: $D_C(T) = U_C k T$. Here k = Boltzmann constant ($J \cdot K^{-1}$), U_C = mobility of diffusing particles, is the coefficient of proportionality between the particle velocity and the driving force (Pa·s·m). If the particles are spherically symmetrical, then $U_C = 1/(6\pi hr)$, where h = the liquid viscosity coefficient, r = radius of the particle [BOMBA, SAFONYK 2013]. Numerical expressions for calculation are also proposed η by BOMBA *et al.* [2016]. $\Phi = \frac{It}{V_A n F} + k_h S_k t$ = the function responsible for the electrochemical reaction, where V_A = device volume (m^3), n = the number of reaction electrons, F = Faraday constant ($C \cdot mol^{-1}$), k_h = the speed constant of the heterogeneous reaction ($mol \cdot (dm^3 \cdot s)^{-1}$), S_k = cathode area (m^2).

To study the model problem (1)–(2) we use the pdepe application of the Matlab software environment, which makes it possible to find the solution of parabolic and elliptical equations, and to explore the influence of parameters in these systems. To obtain a solution based on the pdepe application, it is needed to make four files that describe: a given system of equations (pdex2pde.m), initial conditions (pdex2ic.m), boundary conditions (pdex2bc.m) and the main function (main.m). In the file pdex2pde.m first convert the system of Equations (3) into machine code:

$$\begin{cases} \frac{\partial C}{\partial t} = -v_C \nabla C + \nabla(D_C(T) \nabla C) + f_C(T)C + \Phi \\ \frac{\partial T}{\partial t} = -v_T \nabla T + D_T T + \Psi \end{cases} \quad (3)$$

$$c \left(x, t, u, \frac{\partial u}{\partial x} \right) \frac{\partial u}{\partial t} = x^{-m} \frac{\partial}{\partial x} \left(x^m f \left(x, t, u, \frac{\partial u}{\partial x} \right) \right) + s \left(x, t, u, \frac{\partial u}{\partial x} \right)$$

The contents of the m-file coagul_pdex2pde.m are presented in Figure 1.

```
function [c, f, s] = coagul_pdex2pde(x, t, u, DuDx)
n=0.8; Rg=8.31; I=70;
F=96500; db=1.5*10^-6; As=15; p=101325;
a=0.00012; Lm=0.39*10; L=0.4; U=24; qv=1; c=3310; po=1060;

V1=0;
D1=10^-9;

c1=1; c2=1/a; f1=D1*DuDx(1)-V1*u(1); f2=Lm/L*DuDx(2);

s1=(n*3*Rg*u(2)*I/(8*F*db*As*P)/2.9/(10^-2*(t+1)))*u(1);
s2=I*U*exp(8.8/(0.01*t+1))/(c*po*a);
c = [c1; c2];
f = [f1; f2];
s = [s1; s2];
end
```

Fig. 1. Screenshot of the program code of the file coagul_pdex2pde.m; source: own elaboration

Initial conditions:

$$\begin{cases} C_0(x, t_0) = 0.1, \\ T_0(x, t_0) = 20, \end{cases} \Leftrightarrow u(x, t_0) = u_0(x) \quad (4)$$

The content of the m-file coagul_pdex2ic.m is presented in Figure 2.

```
function u0 = coagul_pdex2ic(x)
u10=0.1;
u20=20;
u0 = [u10;u20];
end
```

Fig. 2. Screenshot of the program code of the file coagul_pdex2ic.m; source: own elaboration

Boundary conditions:

$$\begin{cases} \frac{\partial C^0(x_L, t)}{\partial x} = 0, & \frac{\partial C^0(x_R, t)}{\partial x} = 0, \\ \frac{\partial T^0(x_L, t)}{\partial x} = 0, & \frac{\partial T^0(x_R, t)}{\partial x} = 0, \end{cases} \Leftrightarrow \quad (5)$$

$$p(x, t, u) + q(x, t) \cdot f(x, t, u, \frac{\partial u}{\partial x}) = 0.$$

The content of the m-file coagul_pdex2bc.m is presented in Figure 3.

```
function [p1,q1,pr,qr] = coagul_pdex2bc(xl, ul, xr, ur, t)
p1=[0;0];
q1=[1;1];
pr=[0;0];
qr=[1;1];
end
```

Fig. 3. Screenshot of the program code of the file coagul_pdex2bc.m; source: own elaboration

To describe the main function of pdepe, we use the m-file coagul_pdepe.m, which is presented in Figure 4.

```
m=0;
x=linspace(0,0.6,101);
t=linspace(0,250,101);

sol = pdepe(m, @coagul_pdex2pde, @coagul_pdex2ic, @coagul_pdex2bc, x, t);
u1 = sol(:, :, 1);
u2 = sol(:, :, 2);
```

Fig. 4. Screenshot of the program code of the file coagul_main.m; source: own elaboration

RESULTS AND DISCUSSION

Simulation results for the following input data:

$v = 0.12 \text{ m} \cdot \text{s}^{-1}$; $\eta = 0.8$; $A_s = 15 \text{ m}^2$; $R_g = 8.31 \text{ J} \cdot (\text{mol} \cdot \text{K})^{-1}$; $U = 24 \text{ V}$; $F = 9.65 \cdot 10^4 \text{ C} \cdot \text{mol}^{-1}$; $d_b = 1.5 \cdot 10^{-6} \text{ m}$; $a = 0.12 \cdot 10^{-3} \text{ m}^2 \cdot \text{s}^{-1}$; $\lambda_m = 0.39 \text{ W} \cdot (\text{m} \cdot \text{s})^{-1}$; $a_2 = 880$; $\lambda = 0.4 \text{ W} \cdot (\text{m} \cdot \text{s})^{-1}$; $a_1 = 290$; $c = 3.31 \cdot 10^3 \text{ J} \cdot \text{kg}^{-1}$; $\zeta = 1060 \text{ kg} \cdot \text{mm}^{-3}$; $D = 10^{-9} \text{ m}^2 \cdot \text{s}^{-1}$, are presented in Figure 5.

To study the impact of current on the concentration of ferric iron, we use the results of computer simulations based on problems (1)–(2). In this case, the parameters of the model include: the magnitude of the applied voltage, structural dimensions of the reactor, water characteristics, whereas the simulation time is left constant. By changing the magnitude of the current, we obtained different changes in water temperature and concentration of ferric iron. The obtained results are presented in Figure 6.

In accordance with the set goal, the structure of the laboratory installation for the study of electrocoagulation was

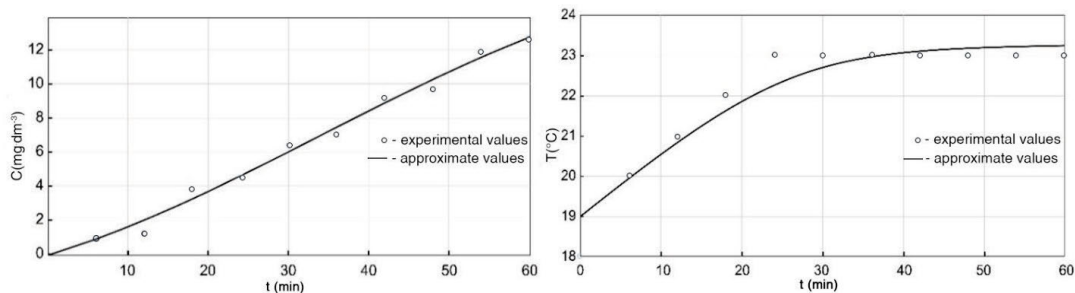


Fig. 5. Distribution: a) the concentration of ferric iron (c) over time at the output of the coagulator; b) water temperature over time; source: own study

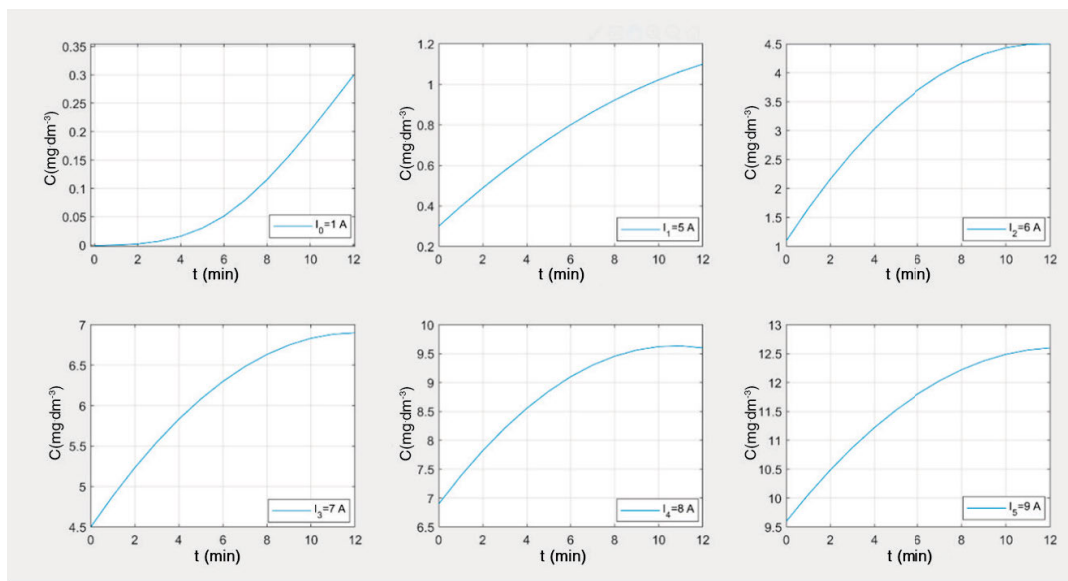


Fig. 6. The change in the concentration of iron (c) at the output of the coagulator over time at the electric current: $I_0 = 1$ A, $I_1 = 5$ A, $I_2 = 6$ A, $I_3 = 7$ A, $I_4 = 8$ A, $I_5 = 9$ A; source: own study

developed, which is shown in Figure 7. The structure uses a flow type electrocoagulator (3) and a container made of non-conductive material with metal plates of different polarity as cathodes and anodes. The electrocoagulator is powered by a laboratory power supply (1). Water is supplied by means of a pump (2), and it is evenly distributed between the coagulator chambers and discharged by means of a pump (4) to the measuring cell (7). The temperature of the environment is monitored using an electronic thermometer (5), which is duplicated by a laboratory one (mercury). The measuring cell consists of a transparent container (8), light source (6), and a sensing element (9). The measurement information and control signals are commutated in the control and registration unit (10). The developed laboratory device allowed to carry out experimental research to check the adequacy of the mathematical model and to obtain additional data on water colour change depending on the iron concentration. According to the plan of the experiment, the coagulation reaction lasted 60 min, and every 6 min the data about the power supply current of the coagulator, temperature and the colour intensity of red, green and blue light components were collected. Thus, 10 samples of a water solution of iron were taken to determine the concentration by standardised methods in a laboratory.

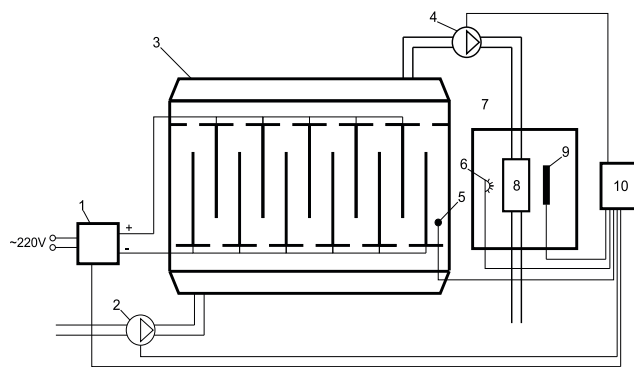


Fig. 7. The laboratory-based automated system for electrochemical production of coagulant using the photocolorimetric analysis; source: own study

Table 1 shows results of an experiment that determined the concentration of total and ferric iron, current and colour of the substance at different times and at variable voltage.

The experimental study was conducted for 60 min. Results obtained show that with the increase in voltage from 5 to 9 V, the current increases from 0.8 to 2.1 A, as shown in Table 1, and the colour of the starting material changes as shown in Figure 8. At the lowest voltage, we can observe the lightest and almost transparent water, whereas at the highest voltage, water becomes turbid and red.

Table 1. Experimental data

Sample No.	Time (min)	Voltage (V)	Current (A)	Colour			Temperature (°C)	Concentration (mg·dm ⁻³)	
				red	green	blue		total iron	Fe ³⁺
1	6	5	0.80	204	207	200	20	0.8	0.33
2	12	5	0.85	214	215	193	22	1.1	0.4
3	18	6	1.30	211	194	75	23	3.7	2.9
4	24	6	1.30	220	173	54	23	4.5	3.1
5	30	7	1.65	210	155	49	23	6.3	5.4
6	36	7	1.65	215	147	41	23	6.9	5.8
7	42	8	1.90	193	116	38	23	9.1	7.1
8	48	8	1.90	189	111	33	23	9.6	7.6
9	54	9	2.05	188	100	27	23	11.8	8.9
10	60	9	2.10	178	74	11	23	12.6	9.6

Source: own study.

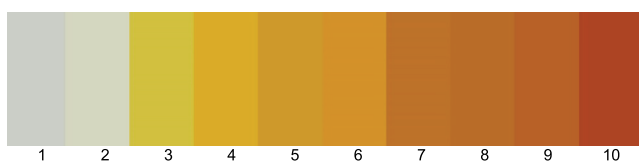


Fig. 8. Substance colour changes with voltage; source: own study

During the study, 10 samples were taken, which are shown in Figure 9, and they helped to determine total iron and ferric Fe³⁺ with the use of KFK2-MP.

While processing the results, graphical dependences were found for the RGB components of water colour and the corresponding concentration of total iron and Fe³⁺ in water (Fig. 10).

By analysing these dependencies of colour components and the concentration, we can conclude that these parameters show stable correlations. Thus, it is possible to develop new rapid methods to assess the concentration of iron in water in real-time,

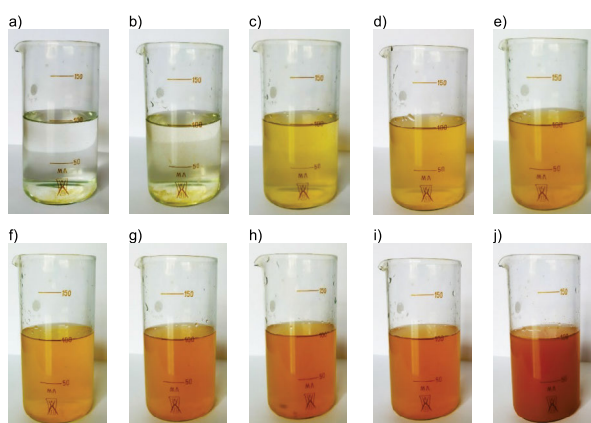


Fig. 9. RGB water colour at variable concentration and experiment time: a) RGB (204; 207; 200), $c = 0.8 \text{ mg}\cdot\text{dm}^{-3}$, $t = 6 \text{ min}$; b) RGB (214; 215; 193), $c = 1.1 \text{ mg}\cdot\text{dm}^{-3}$, $t = 12 \text{ min}$; c) RGB (211; 194; 75), $c = 3.7 \text{ mg}\cdot\text{dm}^{-3}$, $t = 18 \text{ min}$; d) RGB (220; 173; 54), $c = 4.5 \text{ mg}\cdot\text{dm}^{-3}$, $t = 24 \text{ min}$; e) RGB (210; 155; 49), $c = 6.3 \text{ mg}\cdot\text{dm}^{-3}$, $t = 30 \text{ min}$; f) RGB (215; 147; 41), $c = 6.9 \text{ mg}\cdot\text{dm}^{-3}$, $t = 36 \text{ min}$; g) RGB (193; 116; 38), $c = 9.1 \text{ mg}\cdot\text{dm}^{-3}$, $t = 42 \text{ min}$; h) RGB (189; 111; 33), $c = 9.6 \text{ mg}\cdot\text{dm}^{-3}$, $t = 48 \text{ min}$; i) RGB (188; 100; 27), $c = 11.8 \text{ mg}\cdot\text{dm}^{-3}$, $t = 54 \text{ min}$; j) RGB (178; 74; 11), $c = 12.6 \text{ mg}\cdot\text{dm}^{-3}$, $t = 60 \text{ min}$; source: own study

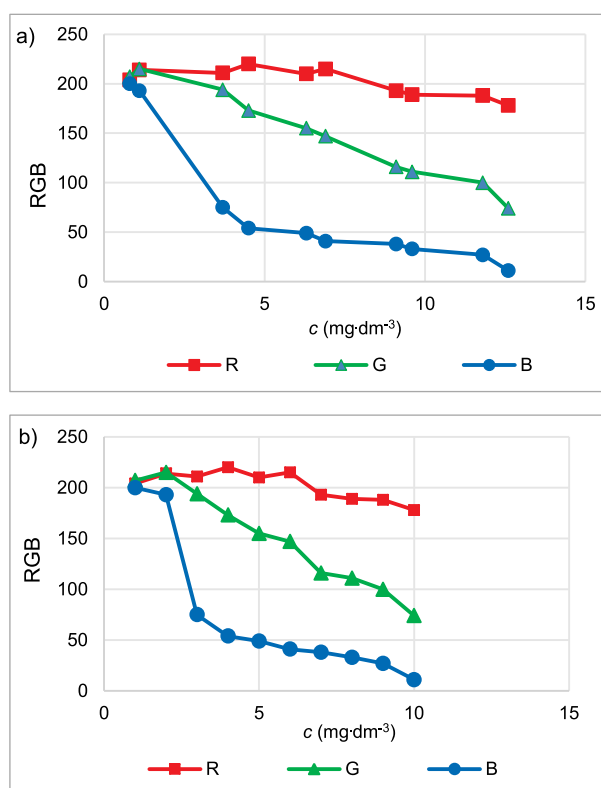


Fig. 10. Dependence of concentration of two iron's forms (c) and RGB components of water colour (10 experimental samples): a) total iron, b) Fe³⁺; source: own study

without the need for sampling, as well as we can further integrate such methods into systems that control electrocoagulation processes.

CONCLUSIONS

The mathematical model of coagulant production has been generalised, which allows to determine the necessary conditions, e.g. the number of plates, size of the reactor, magnitude of the applied voltage, etc., to obtain a given concentration of iron ions. Using the m-function pdepe of the Matlab software environment, the coagulant production system was modelled. The article shows

results of calculations related to the iron ions concentration distribution and the temperature of the aqueous medium at different values of current between the cathode and anode.

The laboratory-scale plant of the iron-containing coagulant based on photocolometric analysis was developed. It consists of a flowing opaque cell through which water is pumped at a constant flow and a module for processing and storage of information. That allows us to reduce human engagement in measurement and to ensure the continuity of the measurement process, especially that sampling of the test material is no longer needed. Moreover, we can also reduce the cost of the measurement process.

REFERENCES

- AL-BARAKAT H.S., MATLOUB F.K., AJAM S.K., AL-HATTAB T.A. 2020. Modeling and simulation of wastewater electrocoagulation reactor. The First International Conference of Pure and Engineering Sciences (ICPES2020). Karbala, Iraq, 26–27.02.2020. IOP Conference. Ser. Materials Science and Engineering. Vol. 871, 012002 p. 1–16. DOI 10.1088/1757-899X/871/1/012002.
- ANNEM S. 2017. Determination of iron content in water. Capstone Project. MSc Thesis. Governors State University OPUS Open Portal to University Scholarship pp. 18.
- ASSÉMIAN A.S., KOUASSI E.K. 2018. Removal of a persistent dye in aqueous solutions by electrocoagulation process: Modeling and optimization through response surface methodology. Water Air and Soil Pollution. Vol. 229(6), 184. DOI 10.1007/s11270-018-3813-2.
- BARRAS J.A.V.A., MOREIRA F., SANTOS G., WISNIEWSKI C., LUCCAS P.O. 2016. Digital image analysis for the colorimetric determination of aluminum, total iron, nitrite and soluble phosphorus in waters. Analytical Letters. Vol. 50(2) p. 414–430. DOI 10.1080/00032719.2016.1182542.
- BOMBA A., KLYMIUK YU., PRYSIAZHNIUK I., PRYSIAZHNIUK O., SAFONYK A. 2016. Mathematical modeling of wastewater treatment from multicomponent pollution by using microporous particles. AIP Conference Proceedings. Vol. 1773, 040003 p. 1–11. DOI 10.1063/1.4964966.
- BOMBA A., SAFONYK A. 2013. Mathematical modeling of aerobic wastewater treatment in porous medium. Zeszyty Naukowe WSInf. Vol. 12. Nr 1 p. 21–29.
- FIRDAUSA M., ALWIB W., TRINOVELDIB F., RAHAYUC I., RAHMIDARD L., WARSITOA K. 2014. Determination of chromium and iron using digital image-based colorimetry. Procedia Environmental Sciences. Vol. 20 p. 298–304. DOI 10.1016/j.proenv.2014.03.037.
- FORERO G., HERNÁNDEZ-LARA R., ROJAS O. 2020. Development of an electrocoagulation equipment for wall paint wastewater treatment. Ingeniería y Competitividad. Vol. 22(2) p. 1–10. DOI 10.25100/iyv.v22i2.9474.
- GOVINDAN K., ARUMUGAM A., KALPANA M., RANGARAJANB M., SHANKARE P., JANG A. 2019. Electrocoagulants characteristics and application of electrocoagulation for micropollutant removal and transformation mechanism. ACS Applied Materials & Interfaces. Vol. 12(1) p. 1775–1788. DOI 10.1021/acsami.9b16559.
- KAUR R., AMIT A. 2018. Treatment of waste water through electrocoagulation. Pollution Research. Vol. 37(2) p. 394–403.
- KHANDEGAR V., ACHARYA S., JAIN A.K. 2018. Data on treatment of sewage wastewater by electrocoagulation using punched aluminum electrode and characterization of generated sludge. Data in Brief. Vol. 18 p. 1229–1238. DOI 10.1016/j.dib.2018.04.020.
- KOYUNCU S., ARIMAN S. 2020. Domestic wastewater treatment by real-scale electrocoagulation process. Water Science and Technology. Vol. 81(4) p. 656–667. DOI 10.2166/wst.2020.128.
- LUKA G. S., NOWAK E., KAWCHUK J., HOORFAR M., NAJJARAN H. 2017. Portable device for the detection of colorimetric assays. Royal Society Open Science. Vol. 4(11), 171025 p. 1–13. DOI 10.1098/rsos.171025.
- MASAWAT P., HARFIELD A., SRIHIRUN N., NAMWONG A. 2016. Green determination of total iron in water by digital image colorimetry. Analytical Letters. Vol. 50(1) p. 173–185. DOI 10.1080/00032719.2016.1174869.
- PAVÓN T., MUNGUÍA G., MOKHTAR A., ROMERO H., HUACUZ J. 2018. Photovoltaic energy-assisted electrocoagulation of a synthetic textile effluent. International Journal of Photoenergy. Vol. 3 p. 1–9. DOI 10.1155/2018/7978901.
- PERREN W., WOJTASIK A., CAI Q. 2018. Removal of microbeads from wastewater using electrocoagulation. American Chemical Society Omega. Vol. 3 p. 3357–3364. DOI 10.1021/acsomega.7b02037.
- POSAVČIĆ H., HALKIJEVIĆ I., VUKOVIĆ Ž. 2019. Application of electrocoagulation for water conditioning. Environmental Engineering – Inženjerstvo Okoliša. Vol. 6. No. 2 p. 59–70. DOI 10.37023/ee.6.2.3.
- RAHMAN A.N., KUMAR N.K.M.F., GILAN U.J., JIHED E.E., PHILIP A., LINUS A.A., SHAHINAN NEN D., ISMAIL V. 2020. Kinetic study & statistical modelling of Sarawak Peat Water Electrocoagulation System using copper and aluminium electrodes. Journal of Applied Science & Process Engineering. Vol. 7(1) p. 439–456. DOI 10.33736/jaspe.2195.2020.
- SAMIR A., CHELLIAPAN S., ZURIATI Z., AJEEL M., ALABA P. 2016. A review of electrocoagulation technology for the treatment of textile wastewater. Reviews in Chemical Engineering. Vol. 33 p. 263–292.
- SHANTARIN V.D., ZAVYALOV V.V. 2003. Optimization of processes of electrocoagulation treatment of drinking water. Nauchnye i Tekhnicheskiye Aspekty Okhrany Okruzhayushchey Sredy. No. 5 p. 62–85.
- YASRI N., ARUMUGAM A., KALPANA M., SHU T., FULADPANJEH B., OLDENBURG T., TRIKOVIĆ M., MAYER B., ROBERTS P.L.E. 2017. Electrocoagulation for the treatment of produced water [online]. University of Calgary. [Access 10.01.2021]. Available at: <https://albertainnovates.ca/wp-content/uploads/2019/07/145-Nael-Yasri.pdf>
- YASRI N., HU J., KIBRIA MD. G., ROBERTS P. L. E. 2020. Electrocoagulation separation processes. Multidisciplinary advances in efficient separation processes. Chapter 6. ACS Symposium Series. Vol. 1348 p. 167–203. DOI 10.1021/bk-2020-1348.ch006.
- YAVUZ Y., ÖGÜTVEREN Ü. B. 2018. Treatment of industrial estate wastewater by the application of electrocoagulation process using iron electrodes. Journal of Environmental Management. Vol. 207 p. 151–158. DOI 10.1016/j.jenvman.2017.11.034.